APEM journal
Advances in Production Engineering & Management
Volume 17 | Number 2 | June 2022 | pp 205–218
https://doi.org/10.14743/apem2022.2.431
ISSN 1854-6250
Journal home: apem-journal.org
Original scientific paper

Machinability analysis and multi-response optimization using NGSA-II algorithm for particle reinforced aluminum based metal matrix composites

Umer, U.[a,*], Mohammed, M.K.[a], Abidi, M.H.[a], Alkhalefah, H.[a], Kishawy, H.A.[b]

[a]Advanced Manufacturing Institute, King Saud University, Riyadh, Saudi Arabia
[b]Machining Research Laboratory, University of Ontario Institute of Technology, Oshawa, ON, Canada

ABSTRACT

In this study the effects of reinforcement particle size and cutting parameters on machining performance variables like cutting force, maximum tool-chip interface temperature and surface roughness of the machined surface have been investigated while machining Aluminum based metal matrix composites (MMCs). MMC bars with silicon carbide reinforcement having 10 % volume fraction and particle sizes of 5 μm, 10 μm and 15 μm are machined with poly-crystalline diamond (PCD) inserts. Experiments are performed using central composite design (CCD) having four parameters with three levels. Response surfaces for each performance variables are generated using polynomial models. Single variable and interaction effects have been investigated using principal component analysis and 3D response charts. Multi-response optimization has been performed to minimize surface roughness and maximum tool-chip interface temperature using non-dominated sorting genetic algorithm II (NSGA-II). In addition, constraints have been applied to the optimization search to filter design points with high cutting forces and low material removal rate. Most of the optimal solutions are found to be with moderate cutting speeds, low feed rate and low depth of cuts.

ARTICLE INFO

Keywords:
Metal Matrix Composites (MMC);
Machining;
Reinforcement particle;
Machinability;
Multi-objective optimization;
Non-dominated sorting genetic algorithm (NSGA-II)

**Corresponding author:*
uumer@ksu.edu.sa
(Umer, U.)

Article history:
Received 8 March 2022
Revised 31 August 2022
Accepted 31 August 2022

1. Introduction

1.1 General

Metal matrix composites (MMCs) are gaining popularity in different fields such as automotive, aerospace, biomedical and electronics. They are gradually replacing conventional metals and alloys owing to their superior properties e.g., strength to weight ratio and wear resistance. They are usually made by net-shape manufacturing techniques. However, to obtain the required accuracy and surface finish, secondary processes such as machining cannot be avoided. Machining of MMCs is different and quite challenging as compared to the traditional metals and alloys due to the presence of hard reinforcement particles. The interactions between reinforcement particles and cutting tools result in excessive tool wear. The debonding and fracture of these reinforcement particles leads to poor surface integrity of the machined surface. The choice of optimum cutting parameters becomes more complex and depends on several factors like shape, size, volume fraction and distribution of these reinforcement particles.

There have been many attempts to analyze machinability of particle reinforced MMCs with respect to cutting forces, chip morphology, surface finish, sub-surface damages and tool wear. The effect of reinforcement particle size on tool wear and surface finish was analyzed by Ciftci *et al*. [1] during machining of Aluminum based MMC with silicon carbide reinforcement (Al/SiCp). They utilized both coated and uncoated carbide tools. MMCs were made up of 30 μm, 45 μm and 110 μm particle sizes and volume fraction of 16 %. They reported that both tool wear and surface finish deteriorate with increasing particle size. Similar findings were reported by Kannan *et al*. [2] also while machining Al/Al_2O_3p MMC having different particle sizes and volume fractions. It was noted that high volume fraction of reinforcement particles also results in an increased tool wear that ultimately leads to poorer finish on the machined surface. High volume fraction of reinforcement particles leads to higher frequency of tool-particle interactions which result in accelerated tool wear. In another study Al/SiCp MMC were machined with 5 %, 10 % and 15 % volume fraction. They concluded that machinability of MMC was severely affected by the cutting speed and volume fraction of reinforcement particles [3]. The effects of cutting speed, feed rate, tool inclination angle and volume fraction of reinforcement particles for Al/SiCp MMC using carbide tool were investigated by Joshi *et al*. [4]. They developed a relationship between flank wear and cutting time and showed that the cutting speed and volume fraction of reinforcement particles are mainly responsible for increased tool wear.

Rai *et al*. [5] performed machinability analysis for different reinforcement materials when cutting Aluminum based MMC with TiC, $TiAl_3$ and Si particles. They evaluated cutting forces and surface roughness for each material and compared with the non-reinforced one. MMC with TiC reinforcement are found to be better and showed lowest cutting forces and reduced surface roughness. The authors reported absences of built-up-edge in case of Al/TiCp MMC which results in low tool wear by attrition as compared to other MMCs. The machinability of aluminum based MMC with B_4C reinforcement particles was analyzed by Karakas *et al*. [6]. They investigated the formation of built-up-edge and tool wear while machining with coated and uncoated tungsten carbide tools. Flank wear and BUE formation was found to be significant for uncoated tools at all cutting speeds. Cheung *et al*. [7] studied the effect of volume fraction of reinforcement on the surface roughness of the machined surface. Tool marks and surface roughness are found to increase as volume fraction increases. They suggested that this might be due to the pronounced spring back effect of the tool cutting edge when it strikes to the hard reinforcement particles. The effect of reinforcement particle size was investigated by Chandrasekaran and Johansson [8] and found that for each particle size there is an optimum feed rate and volume fraction of the reinforcement particles. In another research conducted by Xiaoping and Seah [9] both particle size and volume fraction of reinforcement particles are found to be significant for tool life. They reported that there is a critical value of volume fraction for each particle size above which tool wear increases at a rapid rate. This critical volume found to decrease as particle size increases.

According to researchers, surface integrity of the machined MMC is greatly dependent on the size, shape, volume fraction, bonding strength, and distribution pattern of the reinforcement particles. Lin *et al*. [10] reported that a good quality surface is not easier to achieve for MMCs as fractured and debonded reinforcement particles abrade the surface and cutting tool that leads to pits and tool marks on the machined surface. The effects of shape of the reinforcement (particles and whiskers) on the quality of the machined MMC were analyzed by Cheung *et al*. [7] when cutting Al/SiCp MMC using diamond tools. They examined the tool-particle interactions and reported that cut-through particles leave a good surface finish as compared to the debonded particles as later are mainly responsible for cracking and pits on the machined surface. It was noted that the cut-through mechanism is dominant in whiskers as compared to the particle based MMCs.

Sub-surface damages and surface roughness examinations for machining with particle reinforced MMCs were done by El-Gallab and Sklad [11]. They plotted microhardness profiles for the sub-surface damages and showed that damage is mostly located 60 μm to 100 μm beneath the machined surface. Transmission electron microscopic (TEM) examinations revealed that sub-surface damage is associated with piling up of dislocations in smaller grains areas. Dandekar and

Shin [12] developed a 3D finite element (FE) model with cohesive elements to predict sub-surface damage due to particle debonding while machining Al/SiCp MMC. They calculated debonding energy for SiC particles and showed that the damage depth increases with feed rate which also results in higher cutting forces. Machinability analysis for MMCs with different tools was investigated by Hung *et al*. [13]. They measured the sub-surface damage by testing the microhardness of the plastically deformed machined surfaces. Microscopic examinations of the machined surfaces showed that CBN and PCD tools fractured the reinforced particles along their crystallographic planes resulting in low plastic deformation. In contrast machining with other tools resulted in particles debonding resulted in higher sub-surface damage.

Pramanik *et al*. [14] compared residual stresses for the non-reinforced alloy and MMC. It was noted that longitudinal residual stresses for the non-reinforced alloys are tensile in nature and increases with both cutting speed and feed rate. For MMC the residual stresses are found to be compressive and showing very little dependency on the cutting parameters, i.e. almost constant by changing cutting speed and feed rate. As residual stresses in machining are mainly due to plastic deformation and temperature gradients inside the material, these phenomena are somewhat altered by the presence of hard reinforcement particles. From authors perspective this might be due to constrained matrix flow, hammering effect of the reinforcement particles and compression of the matrix between the cutting tool and hard ceramic particles.

The effect of reinforcement particles during MMC machining was studied by Cheung *et al*. [7] using quick stop test. They observed semi-continuous chips and believed that it is a result of reduction in ductility of the matrix due to hard reinforcement particles. It has also been observed that during cutting the reinforcement particles accumulate along the shear plane. The debonding of the particles and stress concentration accelerate the process of crack propagation resulting in serrated or semi-continuous chips [15]. Similar findings are reported in other studies while turning [11, 16] and drilling [17] Al/SiCp MMCs. Olivas *et al*. [18] reported that tensile residual stresses present on the surface of the ductile matrix generated during fabrication of MMC also facilitate this crack propagation/formation of semi-continuous chips.

The relationships between thrust force, torque and tool wear were examined by Morin *et al*. [19] while drilling non-reinforced aluminum alloy and MMC. They reported almost equal thrust force and torque for aluminum alloy and MMC and concluded that it is the matrix which controls the forces and not the particles. Nonetheless, it was noted that the overall force signal profile over the entire cutting length is much dependent on the size, volume and bonding strength of the reinforcement particles. Sikder and Kishawy [20] developed an analytical force model when machining Aluminum based MMCs with different sizes and volume fractions of alumina (Al_2O_3) particles. They showed that debonding energy and hence cutting force increases with particle size due to increase in surface area of the debonding particle. In contrast Sun *et al*. [21] reported reduction in cutting forces while machining Al/SiCp MMC. However, their study focused on comparatively big particle sizes (15 μm to 60 μm) and large volume fractions (20 % to 50 %).

Various optimization techniques have been used by researchers for machining MMCs and other metallic alloys. However evolutionary algorithms and heuristic optimizers are found to be dominant over gradient based methods. Muthukrishnan and Davim [27] did a surface roughness optimization study using analysis of variance(ANOVA) and artificial neural network (ANN). The study showed that feed rate is the dominant factor to control the surface roughness of the machined MMC in comparison to the depth of cut and cutting speed. They suggested the most optimal cutting parameters to minimize surface roughness. Regression model for tool wear was developed by Seeman *et al*. [28] while machining MMC. Built-up edge (BUE) formation was detected at low cutting speeds resulting in high tool wear. Microscopic examination revealed the presence of both abrasive and adhesive wear at low cutting speeds. Flank wear is found to be more dependent on the cutting speed and feed rate as compared to the depth of cut. Second order response surface models for cutting force, power and specific cutting force for machining Al/SiCp MMC were developed by Gaitonde *et al*. [29]. The developed models showed that variation of cutting force with respect to feed rate is almost same for any value of cutting speed. In addition, they found that an increase in cutting speed resulted in reduction of the cutting force. This is found to be more pronounced at higher feed rates in comparison to lower values. Antonio *et al*.

[30] performed optimization using genetic algorithm (GA) considering multiple objectives while machining aluminum based MMC with 20 % volume of SiC reinforced particles. The output variables considered in the study were machining forces, tool wear and surface roughness. All forces are found to increase with the tool wear whilst cutting force showing marked increase. With other parameters kept constant, surface roughness is found to increase with decrease in cutting speed. The optimum cutting parameters reported with cutting speed of 350 m/min, feed rate of 0.1mm/rev and cutting time equals to 19 min.

In view of the above it is evident that machinability studies in MMC involving temperature measurement are rare. In addition, the interaction effects of particle size with cutting parameters are not explicitly presented in the open literature. This study aims to perform machinability optimization for cutting temperatures and surface roughness while machining MMCs with different particle sizes. The interaction effects of particle size and cutting parameters on maximum tool-chip interface temperature, surface roughness of the machined surface and cutting force has been described in details and finally optimum parameters are suggested for each particle size's MMC.

2. Materials and methods

Aluminum based MMC bars of SupremEx® grade supplied by Materion, UK were utilized for turning operations. These composite bars were made using powder metallurgy and mechanical alloying process route and 100 % compaction is achieved using hot isostatic pressing. Reinforcement particles were made of silicon carbide (SiC) having an average size of 5 μm, 10 μm and 15 μm with 10 % volume fraction. A Kistler piezoelectric quartz dynamometer (9257B) was employed for measuring the cutting forces *Fc* during machining of MMCs. Before converting the analog force signals to digital ones, a dual mode charge amplifier (Kistler 5017B) was connected that converts low charge signals to proportional voltage signals. Dynoware® was used to acquire and save the data for further analysis. An Optris 640 thermal imaging camera was selected to capture maximum tool-chip interface temperature *T* during MMC machining. The camera was mounted on the tool-post as shown in the Fig. 1 and it was set to record maximum temperature during the cutting. The surface quality parameter *Ra* of the turned surfaces was measured using a Taylor Hobson Surtronics S100 tester at three locations after each experimental run and the average value was noted. For the design of experiment (DOE) study, a central composite design CCD-25 with four factors and 3 levels was selected for the study. The factors and their levels are shown in Table 1.

Fig. 1 Experimental setup for MMC turning with thermal imaging camera

Table 1 Factors and their levels for the DOE

Factors	Levels		
	0	1	2
Particle size, *p* (μm)	5	10	15
Cutting speed, *v* (m/min)	60	120	180
Feed rate, *f* (mm/rev)	0.1	0.15	0.2
Depth of cut, *d* (mm)	1.0	1.5	2.0

Using DOE results response surfaces are generated based on 2nd degree polynomials for all the three input variables. These response surfaces are used by the optimization solver in order to predict output variables for the experimental runs not available in the DOE matrix. For optimization, Non-dominated Sorting Genetic Algorithm II (NSGA-II) has been utilized [31]. NGSA-II is a fast and elitist genetic algorithm for multi-response optimization. Elitism improves converges and avoids local optima and guides towards the real pareto optimal design points. There are no penalty parameters for constraints implementation. In fact, the method utilizes a modified dominance method to cater for constraint handling. Though other methods can also be utilized and compared with NGSA-II, the main goal of the study is to select and apply an efficient and robust optimization technique that can handle multiple objectives and constraint considering the population size. The optimization work and other statistical analysis are carried with the help of a general purpose optimization software modeFrontier® developed by Esteco [32]. The workflow involving all elements for the optimization problem is shown in Fig. 2. The optimization problem is set to minimize maximum tool-chip interface temperature and surface roughness on the machined surface with the consideration of constraints on cutting force and material removal rate. The optimization problem is illustrated in Table 2.

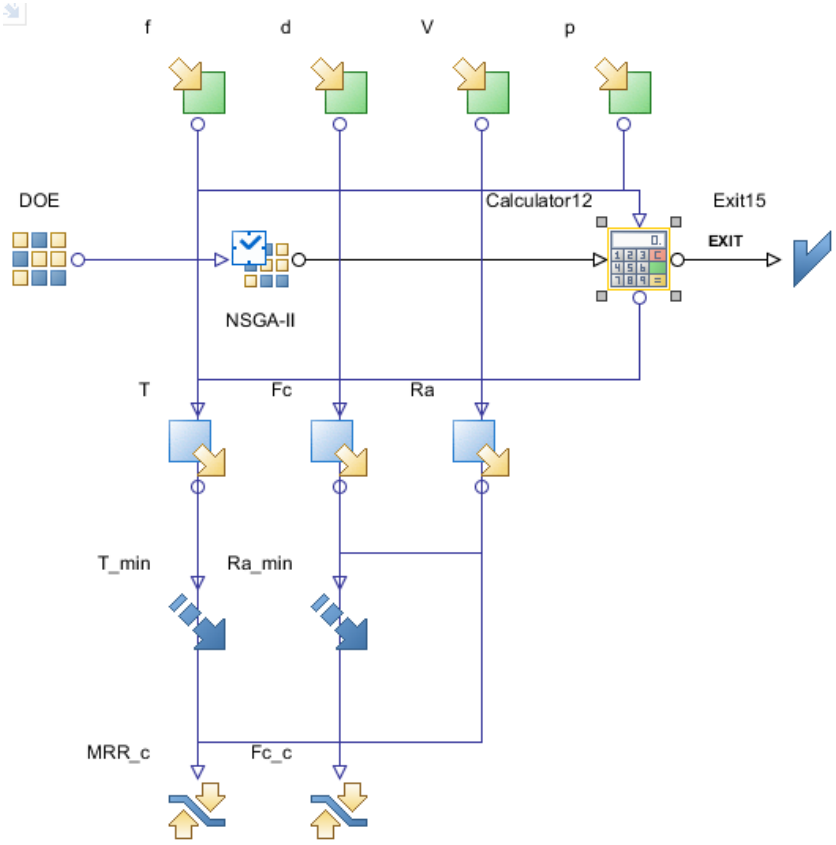

Fig. 2 Optimization workflow with all inputs, outputs, objectives and constraints

Table 2 Optimization problem's objectives and constraints

Objectives	Minimize T Minimize Ra
Constraints	$MRR \geq 200$ mm^3/s $Fc \leq 800$ N

3. Results and discussions

The CCD-25 design matrix with the resulting output variables, i.e. cutting force F_c, maximum tool chip interface temperature T, and surface roughness Ra are shown in Table 3.

Table 3 The CCD-25 design matrix with output variables

Id	*p* (μm)	*v* (m/min)	*f* (mm/rev)	*d* (mm)	*Fc* (N)	*T* (°C)	*Ra* (μm)
0	5	60	0.1	1	287	323.5	2.12
1	5	60	0.2	1	522	393.2	1.62
2	5	60	0.1	2	841	435.2	1.91
3	5	60	0.2	2	1092	466.5	1.52
4	5	180	0.1	1	262	530.3	0.76
5	5	180	0.2	1	489	538.4	1.69
6	5	180	0.1	2	816	610	0.83
7	5	180	0.2	2	1066	698.1	1.69
8	5	120	0.15	1.5	766	543.3	1.18
9	10	60	0.15	1.5	857	407.7	2.53
10	10	180	0.15	1.5	841	638.2	1.53
11	10	120	0.15	1	431	492.9	1.56
12	10	120	0.15	2	1028	581.8	2.04
13	10	120	0.1	1.5	691	529	1.03
14	10	120	0.2	1.5	967	572.4	1.97
15	10	120	0.15	1.5	854	569.2	2.17
16	15	60	0.1	1	357	302.5	1.57
17	15	60	0.2	1	621	392.7	2.53
18	15	60	0.1	2	904	428.5	2.49
19	15	60	0.2	2	1214	537.2	3.07
20	15	180	0.1	1	339	560.1	1.33
21	15	180	0.2	1	598	608.2	2.4
22	15	180	0.1	2	887	732.4	1.9
23	15	180	0.2	2	1196	781.2	2.39
24	15	120	0.15	1.5	864	543.1	2.16

To investigate relationships between input and output variables the spearman's rank correlation coefficient is evaluated and depicted in Fig. 3. It is quite evident that maximum tool-chip interface temperature is highly dependent on cutting speed followed by depth of cut and feed rate. Particle size's effect on temperature is comparatively low but cannot be ignored as tool's crater wear is found to be highly sensitive with respect to maximum tool-chip interface temperature. Surface roughness is found to be severely affected by the size of particle, followed by cutting speed and feed rate. As discussed in the literature review, debonding of particles leave pits and cracks on the machined surface. With large reinforcement particles size of pits increases resulting in poor surface finish. The negative rank for cutting speed indicates reduction in surface roughness with higher cutting speed. This is a common observation in machining as this eliminates BUE resulting in low tool wear and good surface integrity. Finally, the coefficients for cutting force show that it is mainly controlled by depth of cut and feed rate. However the effect of particle size cannot be ignored and the cutting force is found to increase with particle size as observed by Sikder and Kishawy [20]. Cutting force is not much affected by the cutting speed as both strain hardening and thermal softening increases with the cutting speed. Hence both effects neutralize each other.

The interaction effects of the input variables on surface roughness of the machined surface are shown in Fig. 4. The highest interaction effect is provided by feed rate and particle size followed by depth of cut and particle size. With the increase in feed rate, the tool marks on the machined surface becomes more pronounced and hence results in poor surface finish. Similarly due to fracture and debonding of large reinforcement particles, the waviness on the machined surface increases. In contrast the interaction effect of cutting speed and particle size has negligible effect due to their inverse effects on *Ra* when examining individually.

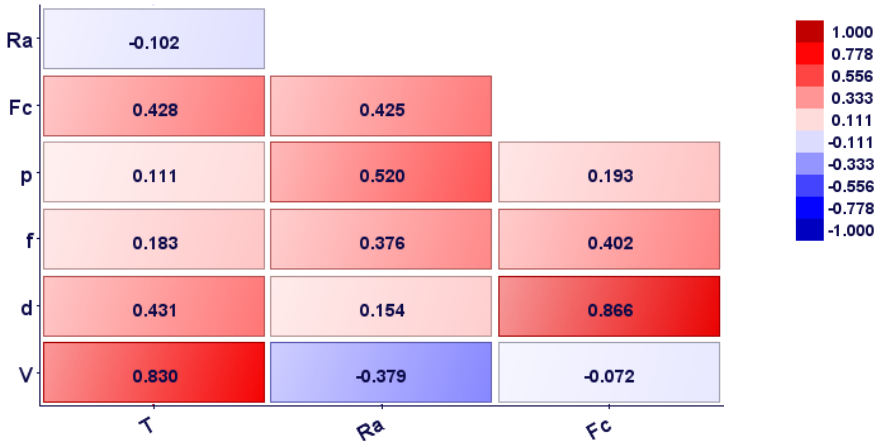

Fig. 3 Spearman's rank correlation matrix

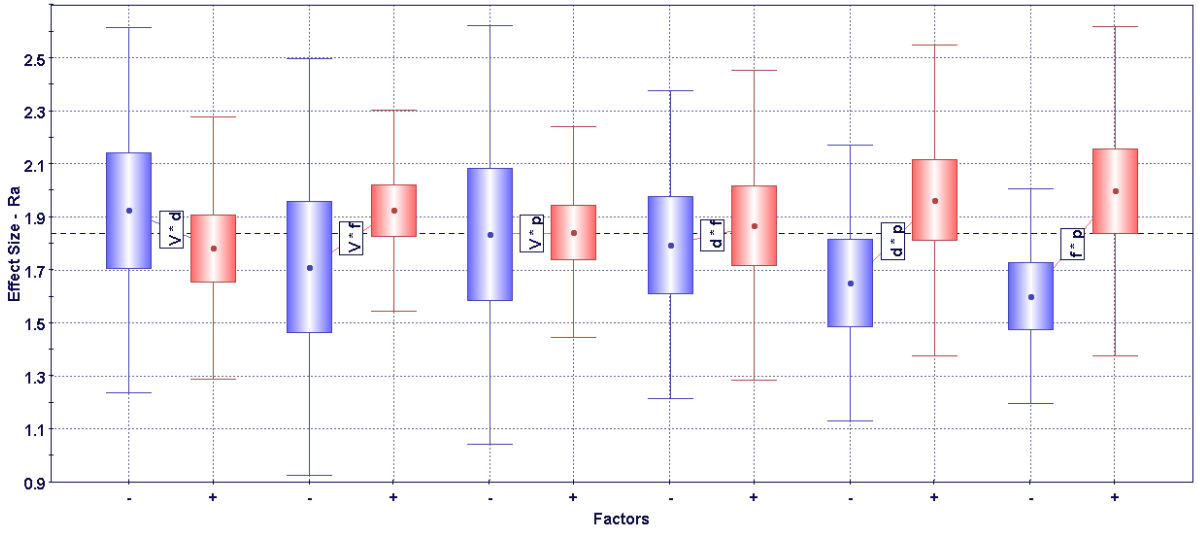

Fig. 4 Interaction effects of input variables on surface roughness

Fig. 5 highlights interaction effect of particle size and cutting parameters on maximum tool-chip interface temperature. The maximum tool-chip interface temperature is an important performance indicator in machining as it is strongly coupled with tool performance and surface integrity of the workpiece. It can be inferred from the figure that maximum interaction effect is provided by the combination of cutting speed and particle size followed by the combination of cutting speed and depth of cut. As it is well known fact in machining that temperatures are mostly affected by cutting speed due to increase in rate of plastic deformation. Hence temperature rises in the primary shear zone. With large reinforcement particles at higher cutting speed, the kinetic energy of the hard reinforcement particles increases [32].This escalates abrasive wear on the cutting tool resulting in higher frictional stresses at the tool-chip interface and hence, temperature rises at the secondary shear zone.

The interaction effects of input variables on cutting force are depicted in Fig. 6. The interaction effect of depth of cut and feed rate is found to be highest followed by the interaction effect of depth of cut and particle size. With the increase in feed rate and depth of cut the chip cross sectional area or the chip load increases on the tool rake face which results in higher cutting and radial forces. In addition, the debonding energy required for the cutting action increases with big sized particles. Similarly, as discussed above tool wear accelerates with increase in particle size. Both phenomena give rise to higher cutting forces.

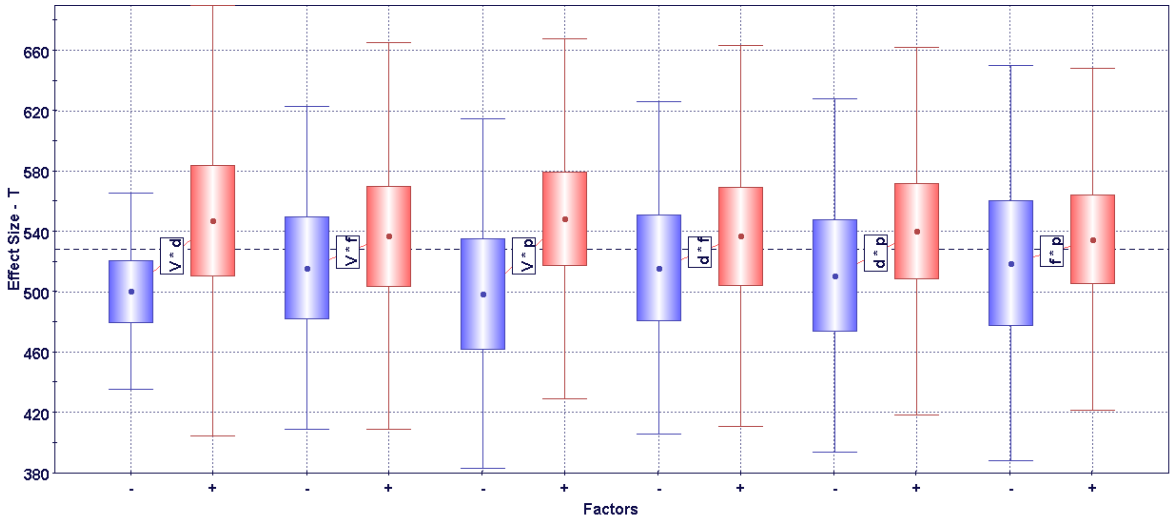

Fig. 5 Interaction effects of input variables on maximum tool-chip interface temperature

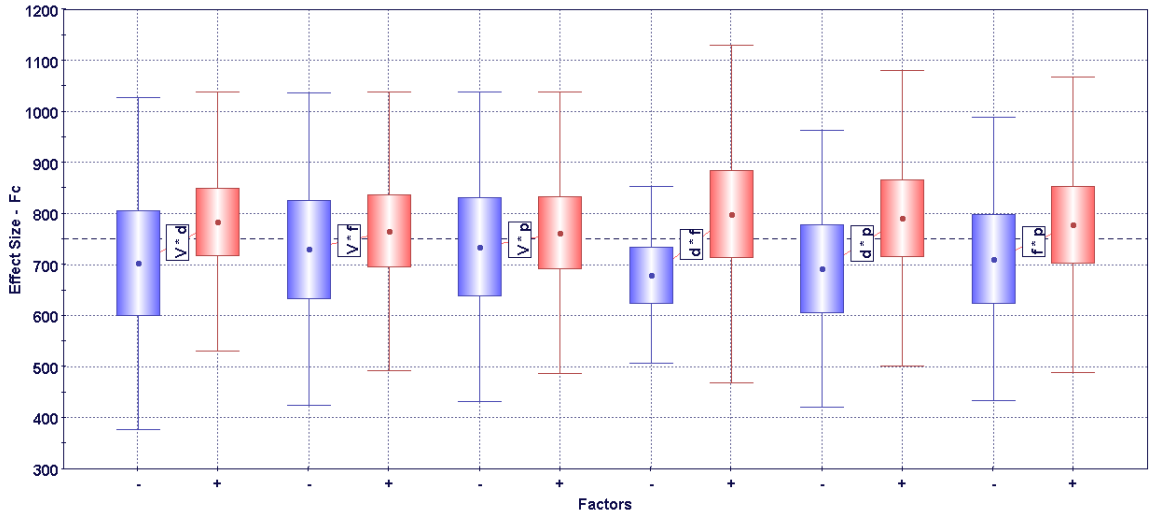

Fig. 6 Interaction effects of input variables on cutting force

The relationships between all the input and output variables can be visualized by principal component analysis as shown in Fig. 7. In this method multidimensional data is reduced to 2 or 3 dimensions of maximum variability called principal components. Here the data is plotted against to principal components *PC*1 and *PC*2 as depicted in Fig. 7. *PC*1 corresponds to 37 % variation in the data whereas *PC*2 corresponds to 28.6 % variation in data. The arrows show the dependency of the input or output variables on the variability of the principal components. Those are collinear with *PC*1 show 100 % dependency and orthogonal ones show null dependency. In this way the relationship between variables could be analyzed by observing their directions or their components in principal directions. It can be seen that *Fc* and *d* have large components along *PC*1. Similarly, *Ra*, *v* and *T* are strongly dependent on *PC*2. As *d* is found to be closer to *Fc* as compared to *f* and p, this suggests a strong correlation between *Fc* and *d*. In this way, *Ra* is found to be more dependent on *p* as compared to *f* and *d*. Also, *T* shows a strong dependency on *v* in comparison to *d* and *f*.

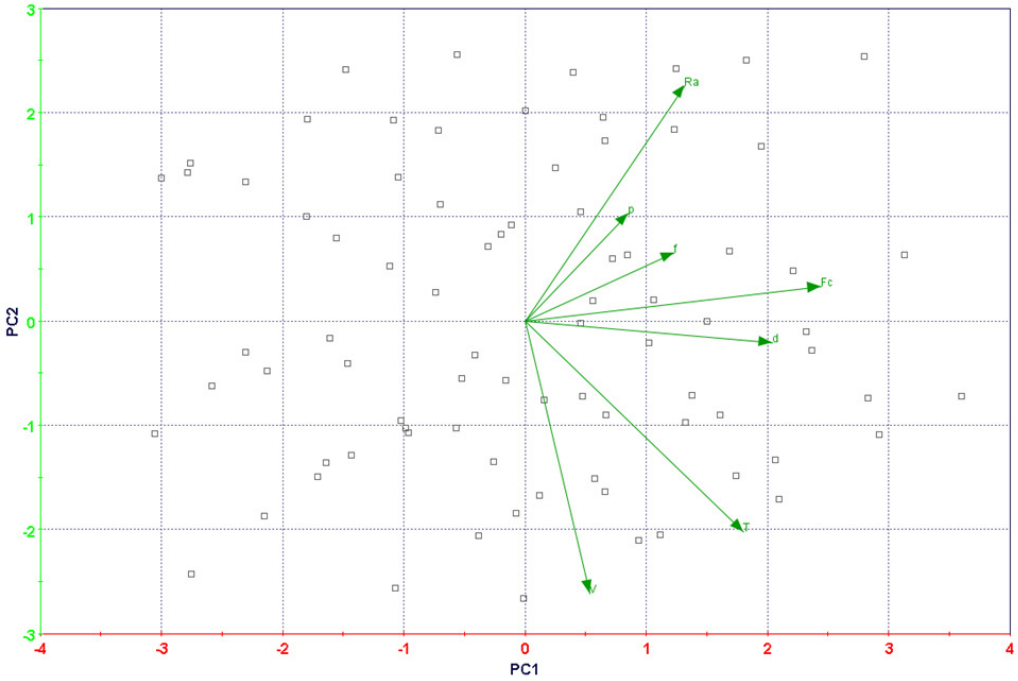

Fig. 7 Principal component analysis (PCA) for all input and output variables

The combined effect of feed rate and reinforcement particle size on surface roughness is shown in Fig. 8. The effect of reinforcement particle size on surface roughness at low feed rate is almost negligible and it increases gradually with feed rate. Similarly with small reinforcement the effect of feed rate on surface roughness is quite low. However, it is increasing with particle size and marked increase in surface roughness can be observed with particle size of 15 μm. Thus, maximum surface roughness is found to be with large reinforcement particles and higher feed rates. Feed marks parallel to the direction of the cutting velocity are more pronounced with increasing feed rate. Also, it has been observed that the reinforcement particles are partially or totally fractured or debonded from the machined surface during cutting. This aggravates further with large reinforcement particles, thus results in poor surface finish.

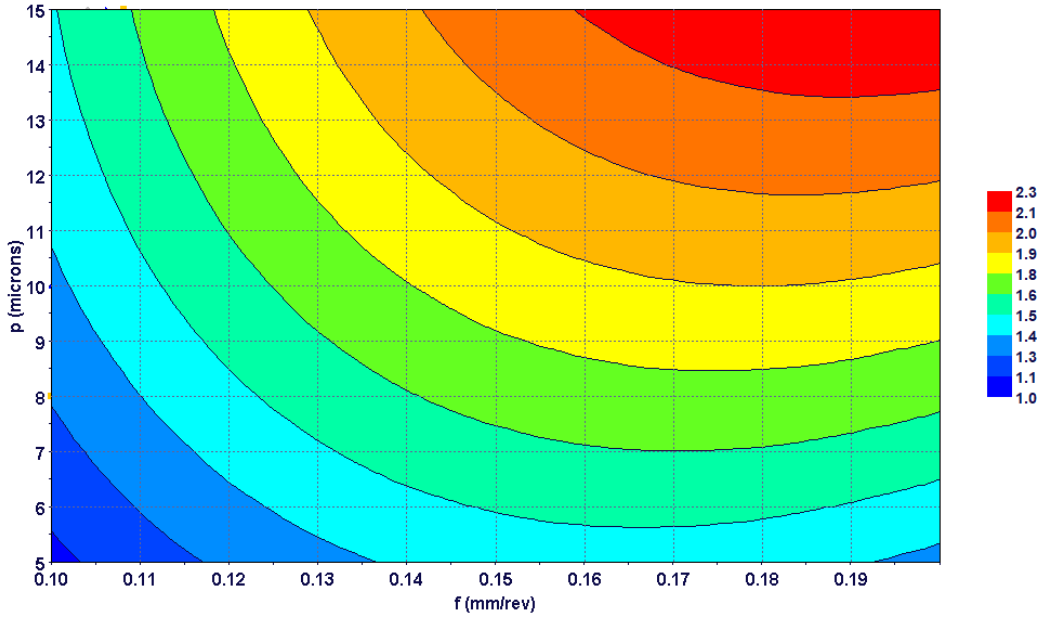

Fig. 8 Effects of feed rate and particle size on surface roughness

Fig. 9 shows the combined effect of depth of cut and reinforcement particle size on cutting force during MMC machining. The effect of reinforcement particle size on cutting force is marginally very low as compared to the depth of cut, though both factors contribute positively as shown in figure. Maximum cutting force is obtained at the top right corner, i.e. with large depth of cut and big reinforcement particles. As cutting force is proportional to the depth of cut due to increase in chip load, the debonding energy increases with particle size that leads to further escalation in cutting force as depicted in Fig. 9.

The combined effect of feed rate and reinforcement particle size on maximum tool-chip interface temperature is shown in Fig. 10. It is depicted that maximum tool-chip interface temperature increases with both feed rate and reinforcement particle size. Increase in particle size at low feed rate results in approximately 5.6 % rise in temperature. Whereas a jump of 8.8 % is observed at higher feed rate as shown in figure. The plastic energy consumed at the primary shear zone is proportional to the uncut chip thickness, i.e. feed rate. Thus, higher feed rates result in high heat dissipation which escalates temperature at the tool-chip interface. Similarly large reinforcement particles give rise to rapid tool wear which increases friction and heat generation at the secondary shear zone, thus resulting in higher tool-chip interface temperature.

Large reinforcement particles are also responsible for high abrasive wear on the tool flank face. This is due to increase in kinetic energy for the large particles which increases their rolling and sliding actions on the tool's surface. Effects of particle size on tool's flank wear can be analyzed in Fig. 11 (Scanning electrons photomicrographs) showing high abrasive wear on tool's flank face with 15 μm MMC. Welded aluminum can be seen on the tool's edges as it is a common problem when machining at dry conditions with higher speeds and low feed rates.

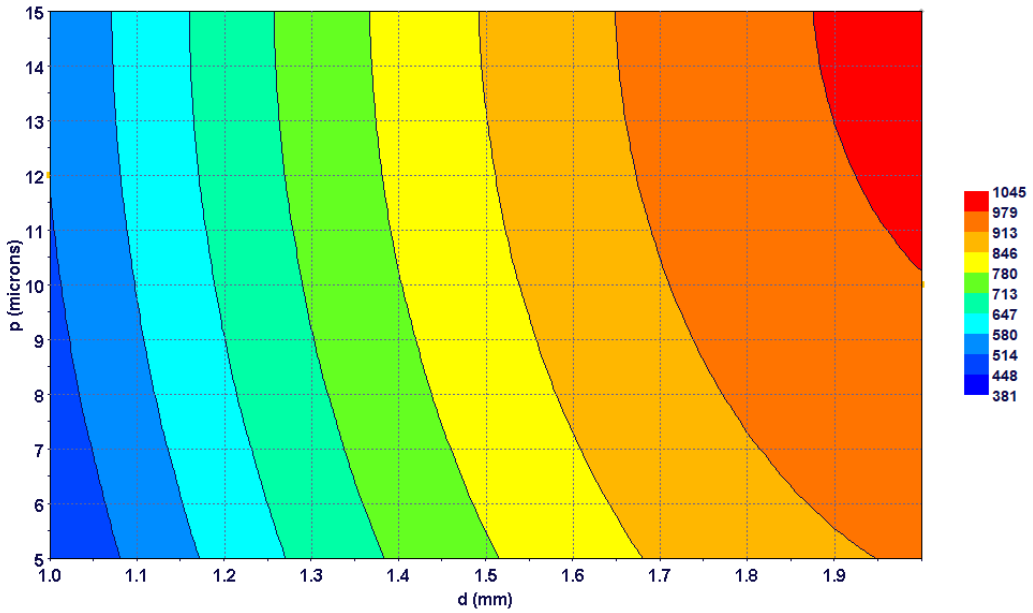

Fig. 9 Effects of depth of cut and particle size on cutting force

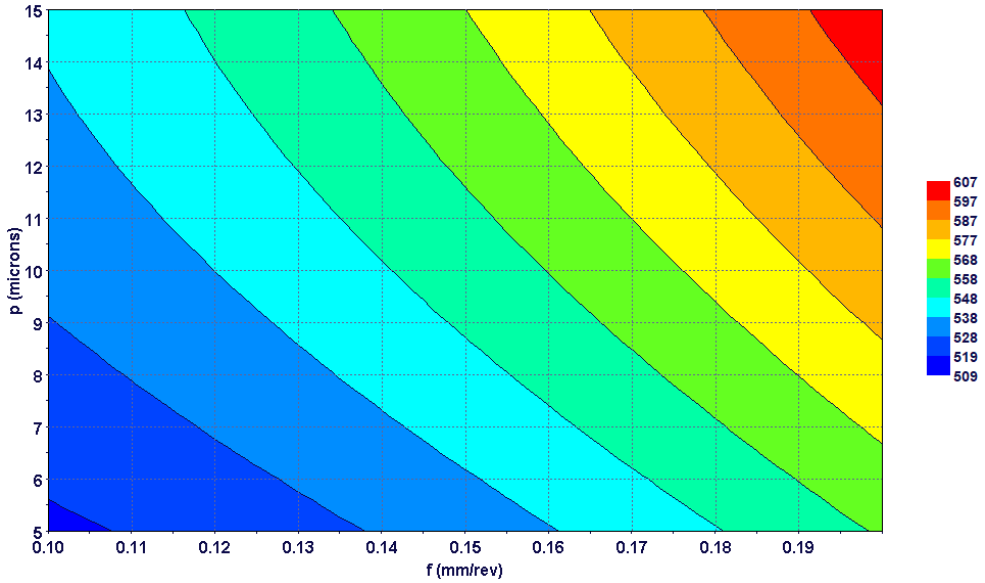

Fig. 10 Effects feed rate and particle size on maximum tool-chip interface temperature

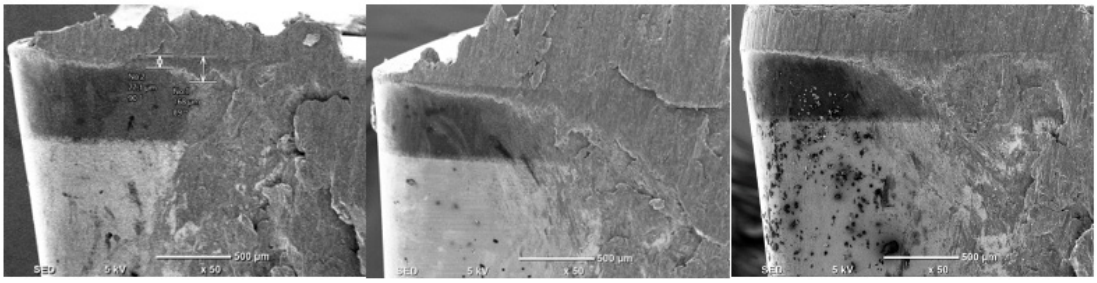

(a) (b) (c)

Fig. 11 Tool wear when machining MMC: (a) 5 μm, (b) 10 μm, (c) 15 μm
v = 180 m/min, f = 0.10 mm/rev, d = 1.0 mm, cutting time = 10 min

All the experimental runs obtained after optimization are shown in a 3D bubble chart as illustrated in Fig. 12. They are plotted against the two objectives, i.e. surface roughness *Ra* and maximum tool chip interface temperature *T*. The size of the bubble indicates reinforcement particle size. The design points with yellow colors are considered as unfeasible, i.e. violating at least one constraint in the optimization problem. The solid ones are said to be real as they are from the DOE matrix, whereas hollow bubbles represent virtual design point obtained via response surfaces. As the objective is to minimize both surface roughness and maximum tool-chip interface temperature, the optimal design points should be at the lower left corner of the diagram. A pareto-front can be drawn for each particle size to find out the optimal design points. Using the pareto front for 5 μm particle size three design points A5, B5 and C5 can be marked as candidates for optimal solution. Similarly, A10 and B10 can be marked as optimal for 10 μm particle size MMC. For 15 μm MMC, only one feasible design point is found in the optimal area and marked as A15 as shown in figure. The feasible design points marked with letter B are characterized by low feed rate, low depth of cut and moderate cutting speed. Similarly design point A5 have higher cutting speed and relatively higher MMR as compared to design points B5. The details of all the possible optimal solutions are shown in Table 4.

The relationship between four variables at a time can be visualized by a 4D bubble chart as shown in Fig. 13. Similar to the 3D bubble chart as explained above, the design points are plotted against the two objectives *Ra* and *T*. Cutting speed v is represented by color of the bubble whereas feed rate f is represented by the size of the bubble. It can be seen that higher temperatures are mostly contributed by high cutting speed and high interactions effects of the remaining input variables, i.e. $f \cdot d$, $f \cdot p$ and $d \cdot p$. Similarly poor surface finish is found to be associated with low cutting speed, moderate and high feed rate or depth of cut and large reinforcement particles.

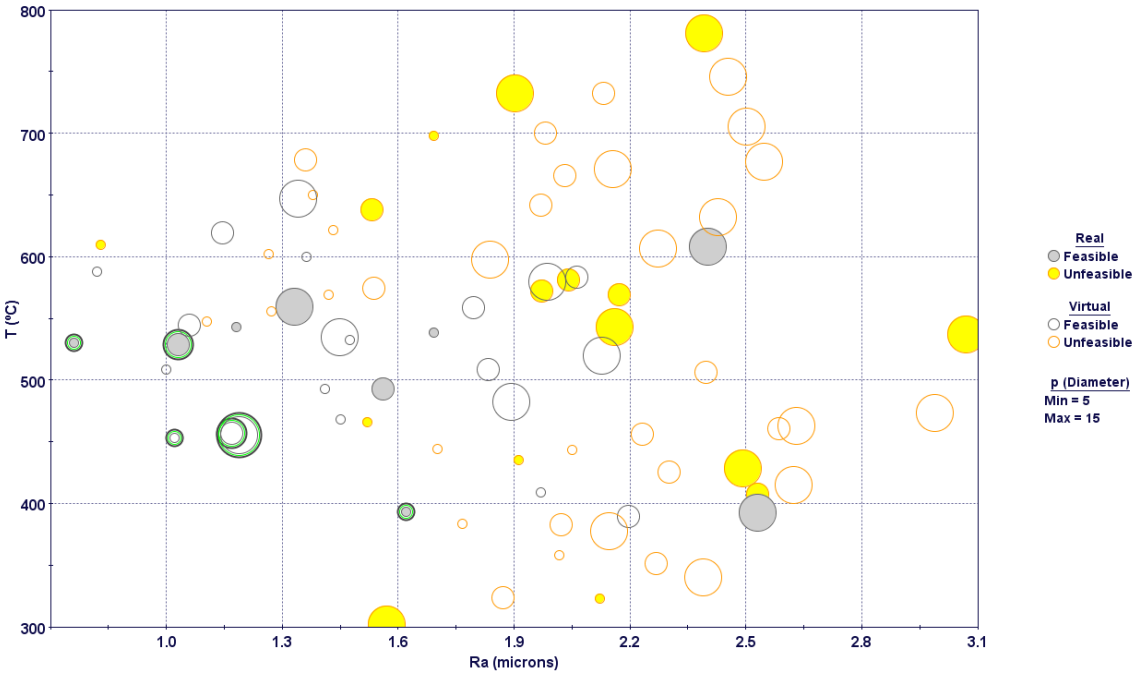

Fig. 12 3D bubble charts showing design points against the two objectives

Table 4 Details of optimal solutions

Id	p (μm)	v (m/min)	f (mm/rev)	d (mm)	F_c (N)	T (°C)	Ra (μm)
A5	5	180	0.1	1.0	262	530.3	0.76
B5	5	120	0.1	1.0	262	453.5	1.02
C5	5	60	0.2	1.0	522	393.2	1.62
A10	10	120	0.1	1.5	691	529.0	1.03
B10	10	120	0.1	1.0	316	457.1	1.17
A15	15	120	0.1	1.0	329	455.8	1.19

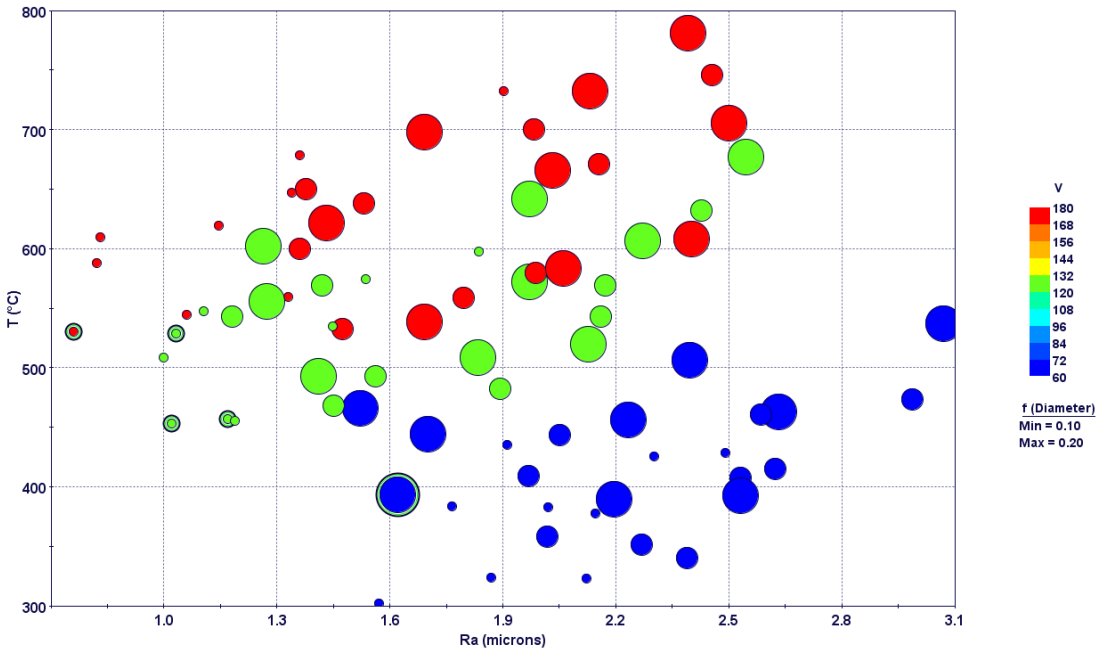

Fig. 13 4D bubble charts showing design points with four variables at a time

4. Conclusions

Machinability analysis and multi-objective optimization for particle reinforced aluminium based MMC have been performed during machining with PCD inserts. Effects of particle size on cutting force, surface roughness and maximum tool-chip interface temperature have been investigated with some qualitative analysis for the flank wear on PCD inserts. Following conclusions can be drawn:

- It has been noticed that particle size main and interaction effects contribute significantly towards the machinability of particle reinforced aluminium based MMCs.
- Surface roughness of the machined MMCs is found to be highly affected by the size of the reinforcement particles. Large reinforcement particles lead to poorer surface finish.
- As feed rates increase surface roughness more aggressively than other cutting parameters, the highest interaction effect is provided by the combination of particle size and feed rate.
- Large reinforcement particles are also found responsible for higher cutting temperatures. The interaction effect of cutting speed and particle size is found to be significant in controlling the maximum tool-chip interface temperature.
- Cutting force is found to be mainly influenced by depth of cut and feed rate. Particle size effect is found to be low for the volume fraction selected in the study. However, its effect cannot be ignored when other parameters are kept constant.
- The interaction effect of depth of cut and particle size is found significant for the cutting force. The debonding energy of the reinforced particles increases with size during machining. Hence results in escalation of the cutting force.
- Most of the optimal solutions are found to be with moderate cutting speed, low depth of cut and low feed rates.

Acknowledgement

This project was funded by the National Plan for Science, Technology, and Innovation (MAARIFAH), King Abdulaziz City for Science and Technology, Kingdom of Saudi Arabia, Award No. 13-ADV-971-02.

References

[1] Ciftci, I., Turker, M., Seker, U. (2004). Evaluation of tool wear when machining SiC_p-reinforced Al-2014 alloy matrix composites, *Materials & Design,* Vol. 25, No. 3, 251-255, doi: 10.1016/j.matdes.2003.09.019.

[2] Kannan, S., Kishawy, H.A., Balazinski, M. (2005). Flank wear progression during machining metal matrix composites, *Journal of Manufacturing Science and Engineering,* Vol. 128, No. 3, 787-791, doi: 10.1115/1.2164508.

[3] Ozben, T., Kilickap, E., Çakır, O. (2008). Investigation of mechanical and machinability properties of SiC particle reinforced Al-MMC, *Journal of Materials Processing Technology,* Vol. 198, No. 1-3, 220-225, doi: 10.1016/j.jmatprotec.2007.06.082.

[4] Joshi, S.S., Ramakrishnan, N., Nagarwalla, H.E., Ramakrishnan, P. (1999). Wear of rotary carbide tools in machining of Al/SiCp composites, *Wear,* Vol. 230, No. 2, 124-132, doi: 10.1016/S0043-1648(99)00092-7.

[5] Rai, R.N., Datta, G.L., Chakraborty, M., Chattopadhyay, A.B. (2006). A study on the machinability behaviour of Al–TiC composite prepared by in situ technique, *Materials Science and Engineering: A,* Vol. 428, No. 1-2, 34-40, doi: 10.1016/j.msea.2005.11.040.

[6] Karakaş, M.S., Acır, A., Übeyli, M., Ögel, B. (2006). Effect of cutting speed on tool performance in milling of B_4C_p reinforced aluminum metal matrix composites, *Journal of Materials Processing Technology,* Vol. 178, No. 1-3, 241-246, doi: 10.1016/j.jmatprotec.2006.04.005.

[7] Cheung, C.F., Chan, K.C., To, S., Lee, W.B. (2002). Effect of reinforcement in ultra-precision machining of Al6061/SiC metal matrix composites, *Scripta Materialia,* Vol. 47, No. 2, 77-82, doi: 10.1016/S1359-6462(02)00097-0.

[8] Chandrasekaran, H., Johansson, J.-O. (1996). On the behaviour of fibre/particle reinforced aluminium alloy matrix composites in milling and grinding, In: *Proceedings of 2nd International Conference on Machining of Advanced Materials,* Aachen, Germay, 463-478.

[9] Li, X., Seah, W.K.H. (2001). Tool wear acceleration in relation to workpiece reinforcement percentage in cutting of metal matrix composites, *Wear,* Vol. 247, No. 2, 161-171, doi: 10.1016/S0043-1648(00)00524-X.

[10] Lin, J.T., Bhattacharyya, D., Ferguson, W.G. (1998). Chip formation in the machining of SiC-particle-reinforced aluminium-matrix composites, *Composites Science and Technology,* Vol. 58, No, 2, 285-291, doi: 10.1016/S0266-3538(97)00126-7.

[11] El-Gallab, M., Sklad, M. (1998). Machining of Al/SiC particulate metal matrix composites: Part II: Workpiece surface integrity, *Journal of Materials Processing Technology,* Vol. 83, No. 1-3, 277-285, doi: 10.1016/S0924-0136(98)00072-7.
[12] Dandekar, C.R., Shin, Y.C. (2009). Multi-step 3-D finite element modeling of subsurface damage in machining particulate reinforced metal matrix composites, *Composites Part A: Applied Science and Manufacturing,* Vol. 40, No. 8, 1231-1239, doi: 10.1016/j.compositesa.2009.05.017.
[13] Hung, N.P., Boey, F.Y.C., Khor, K.A., Phua, Y.S., Lee, H.F. (1996). Machinability of aluminum alloys reinforced with silicon carbide particulates, *Journal of Materials Processing Technology,* Vol. 56, No. 1-4, 966-977, doi: 10.1016/0924-0136(95)01908-1.
[14] Pramanik, A., Zhang, L.C., Arsecularatne, J.A. (2008). Machining of metal matrix composites: Effect of ceramic particles on residual stress, surface roughness and chip formation, *International Journal of Machine Tools and Manufacture,* Vol. 48, No. 15, 1613-1625, doi: 10.1016/j.ijmachtools.2008.07.008.
[15] Iuliano, L., Settineri, L., Gatto, A. (1998). High-speed turning experiments on metal matrix composites, *Composites Part A: Applied Science and Manufacturing,* Vol. 29, No. 12, 1501-1509, doi: 10.1016/S1359-835X(98)00105-5.
[16] Kannan, S., Kishawy, H.A. (2008). Tribological aspects of machining aluminium metal matrix composites, *Journal of Materials Processing Technology,* Vol. 198, No. 1-3, 399-406, doi: 10.1016/j.jmatprotec.2007.07.021.
[17] Tosun, G., Muratoglu, M. (2004). The drilling of an Al/SiC_p metal-matrix composites. Part I: microstructure, *Composites Science and Technology,* Vol. 64, No. 2, 299-308, doi: 10.1016/S0266-3538(03)00290-2.
[18] Olivas, E.R., Swadener, J.G., Shen, Y.-L. (2006). Nanoindentation measurement of surface residual stresses in particle-reinforced metal matrix composites, *Scripta Materialia,* Vol. 54, No. 2, 263-268, doi: 10.1016/j.scriptamat.2005.09.021.
[19] Morin, E., Masounave, J., Laufer, E.E. (1995). Effect of drill wear on cutting forces in the drilling of metal-matrix composites, *Wear,* Vol. 184, No. 1, 11-16, doi: 10.1016/0043-1648(94)06541-1.
[20] Sikder, S., Kishawy, H.A. (2012). Analytical model for force prediction when machining metal matrix composite, *International Journal of Mechanical Sciences,* Vol. 59, No. 1, 95-103, doi: 10.1016/j.ijmecsci.2012.03.010.
[21] Sun, W., Duan, C., Yin, W. (2021). Modeling of force and temperature in cutting of particle reinforced metal matrix composites considering particle effects, *Journal of Materials Processing Technology,* Vol. 290, Article No. 116991, doi: 10.1016/j.jmatprotec.2020.116991.
[22] Klancnik, S., Hrelja, M., Balic, J., Brezocnik, M. (2016). Multi-objective optimization of the turning process using a Gravitational Search Algorithm (GSA) and NSGA-II approach, *Advances in Production Engineering & Management*, Vol. 11, No. 4, 366-376, doi: 10.14743/apem2016.4.234.
[23] Duplak, J., Hatala, M., Duplakova, D., Steranka, J. (2018). Comprehensive analysis and study of the machinability of a high strength aluminum alloy (EN AW-AlZn5.5MgCu) in the high-feed milling, *Advances in Production Engineering & Management*, Vol. 13, No. 4, 455-465, doi: 10.14743/apem2018.4.303.
[24] Xu, E.B., Yang, M.S., Li, Y., Gao, X.Q., Wang, Z.Y., Ren, L.J. (2021). A multi-objective selective maintenance optimization method for series-parallel systems using NSGA-III and NSGA-II evolutionary algorithms, *Advances in Production Engineering & Management*, Vol. 16, No. 3, 372-384, doi: 10.14743/apem2021.3.407.
[25] Aljinović, A., Bilić, B., Gjeldum, N., Mladineo, M. (2021). Prediction of surface roughness and power in turning process using response surface method and ANN, *Tehnički Vjesnik – Technical Gazette*, Vol. 28, No. 2, 456-464, doi: 10.17559/TV-20190522104029.
[26] Can, A., Ünüvar, A. (2017). Optimization of process parameters in drilling of SMC composites using Taguchi method, *Tehnički Vjesnik – Technical Gazette,* Vol. 24, No. 2, 435-442, doi: 10.17559/TV-20160103215256.
[27] Muthukrishnan, N., Davim, J.P. (2009). Optimization of machining parameters of Al/SiC-MMC with ANOVA and ANN analysis, *Journal of Materials Processing Technology,* Vol. 209, No. 1, 225-232, doi: 10.1016/j.jmatprotec.2008.01.041.
[28] Seeman, M., Ganesan, G., Karthikeyan, R., Velayudham, A. (2010). Study on tool wear and surface roughness in machining of particulate aluminum metal matrix composite-response surface methodology approach, *International Journal of Advanced Manufacturing Technology,* Vol. 48, 613-624, doi: 10.1007/s00170-009-2297-z.
[29] Gaitonde, V.N., Karnik, S.R., Davim, J.P. (2009). Some studies in metal matrix composites machining using response surface methodology, *Journal of Reinforced Plastics and Composites*, Vol. 28, No. 20, 2445-2457, doi: 10.1177/0731684408092375.
[30] António, C.A.C., Davim, J.P. (2002). Optimal cutting conditions in turning of particulate metal matrix composites based on experiment and a genetic search model, *Composites Part A: Applied Science and Manufacturing,* Vol. 33, No. 2, 213-219, doi: 10.1016/S1359-835X(01)00094-X.
[31] Deb, K., Pratap, A., Agarwal, S., Meyarivan, T. (2002). A fast and elitist multi-objective genetic algorithm: NSGA-II, *IEEE Transactions on Evolutionary Computation,* Vol. 6, No. 2,182-197, doi: 10.1109/4235.996017.
[32] modeFrontier, from *https://engineering.esteco.com/modefrontier,* accessed February 1, 2022.
[33] Kannan, S., Kishawy, H.A., Deiab, I.M., Surappa, M.K. (2006). On the role of reinforcements on tool performance during cutting of metal matrix composites, *Journal of Manufacturing Processes,* Vol. 8, No. 2, 67-75, doi: 10.1016/S1526-6125(07)00006-0.